Determination of Blood Curve and Tissue Uptake from Left Ventricle Using FADS in Rat FDG-PET Studies[1]

M. Bentourkia, D. Lapointe, V. Selivanov, I. Buvat*, R. Lecomte
Université de Sherbrooke, Sherbrooke, Québec, Canada,
*U494 INSERM, CHU Pitié-Salpêtrière, Paris, France

Abstract

Blood input function is necessary for quantitative pharmacokinetic studies in Positron Emission Tomography (PET). However, external blood sampling from small animals presents many limitations. In this work, we show that the blood input function in rats can be extracted from the left ventricular blood pool using Factor Analysis of Dynamic Structures (FADS). Images of the heart from eight rats were acquired with the Sherbrooke animal PET scanner. A region of interest (ROI) was drawn around the left ventricle (LV) and decomposed into the blood pool and the myocardium tissue using FADS. The input curve (IC) obtained with FADS is comparable to that obtained from measured images for the first frames, while it significantly decreases with increasing time. The myocardium tissue segments present lower amplitude at early times and approximately no change at later times in comparison to the same ROIs obtained from measured images. On average, the variation of the total counts were about 18%, 19% and 43% in the IC, anterior and septal ROIs obtained from images reconstructed with maximum likelihood algorithm. IC and myocardium tissue uptake can be safely obtained from rat heart scans and corrected for spillover using FADS for images obtained with either iterative reconstruction or with the usual filtered backprojection.

I. INTRODUCTION

Small animal positron emission tomography (PET) is a promising technique to study pharmacokinetic and pharmacodynamic behavior of drugs in living bodies. The major limitations encountered are the limited spatial resolution of the scanners in imaging structures of some mm of thickness, and the small signal emitted by these structures as a function of the injected activity. Another difficulty, which is not dependent on the tomograph, is the external blood sampling necessary for quantitative analysis. Small animals such as rats present many limitations in blood extraction. The Sherbrooke animal PET scanner which is based on small and independent detectors ($3 \times 5 \times 20$ mm) [1], achieves a spatial resolution of 2.1 mm in-plane by 3 mm axially and allows the continuous acquisition of image frames of 5 sec or less. These short time frames would permit extraction of the input curve from the left ventricle with sufficient time resolution to measure the peak blood tracer concentration with good accuracy. However, at later times, this input curve is contaminated with activity emitted from the myocardial tissue. In this work, we use the technique of Factor Analysis of Dynamic Structures (FADS) [2], [3], [4] to extract an accurate blood curve and myocardial time activity curves (TACs) corrected for spill-over in rat glucose metabolism studies.

II. MATERIALS AND METHODS

A. Measurements

PET data were collected in 8 rats weighting ~200 gr using FDG. Tracer injection consisted of 2 mCi of FDG in physiological saline solution with a bolus duration of 30 sec. A series of 37 PET image frames over 51 minutes were acquired with the Sherbrooke animal PET tomograph [1] in dynamic mode according to the following sequence:: 24 x 5 sec; 8 x 180 sec and 5 x 300 sec. The reduced frame lengths during the first two minutes allowed adequate sampling of the blood curve to define the peak. External blood sampling was not available. Images were reconstructed using both maximum likelihood (ML) with 30 iterations at 0.42 mm/pixel [5] and the usual filtered backprojection (FBP) methods.

B. Analysis Procedure

In order to decompose the left ventricle dynamic image sequence excluding all other structures and background, the first operation was to manually draw a region of interest (ROI) around the left ventricular tissue on the last frame where the myocardium was clearly defined. The pixels contained in the ROI were rearranged in columns for each frame. They were standardized and centered then FADS procedure was applied with two physiological components. The number of components was justified by the radioactivity uptake in these two regions assuming no contamination from neighboring structures due to the small thickness of the imaged slice (~3mm). No constraints other than non-negativity constraints were used in FADS. For each compartment k, FADS resulted in a factor f_k (dynamic curve of T time points) and a factor image a_k. The normalized factor f_k ($\Box_k f_k(t)=1$) represents the unique TAC associated to the compartment k (i.e., the input curve for the blood pool compartment and the myocardial tissue TAC for the myocardium compartment). The factor image a_k shows the contribution of each pixel i to the compartment k, the pixel intensity a_{ik} being equal to the signal intensity in pixel i explained by that compartment k. Using a factor f_k and its associated factor image a_k, the dynamic image sequence C_{ik} corresponding to a single physiological component k can be calculated using:

$$C_{ik}(t) = a_{ik} f_k(t).$$

1This work was supported in part by the Medical Research Council of Canada under grant MT-15348

Using this equation, a «pure» blood pool image sequence and a «pure» myocardial tissue image sequence were calculated from FADS results. In addition, a blood pool ROI was drawn within the blood pool on the blood pool factor image and 4 myocardial tissue ROIs, corresponding to the anterior, lateral, inferior and septal segments, were drawn on the myocardium factor image.

On the other hand, blood pool TAC and myocardial tissue TACs were obtained from the original dynamic image sequence, by using the 5 ROIs drawn on the factor images. The typical size of these ROIs was made of at least ten pixels.

Comparing the TACs obtained from the pure image sequences with those obtained from the original image sequences allowed us to study the effect of spillover.

III. RESULTS

Figure 1 shows the last frame of the image series reconstructed by ML (Figure 1a) and FBP (Figure 1b) on a 128 × 128 grid. In both images, the right and left ventricle are clearly resolved. A ROI manually drawn around the left ventricular tissue and separated into two structures using FADS generated the images in Figures 2 and 3, for the blood pool and for the myocardium, respectively. The corresponding components obtained from the FBP reconstructed images (Figure 1b) were similar to those in Figures 2 and 3. Two dynamic image sequences were generated from the factor images for blood pool and for myocardium tissue, respectively. To extract the input curve and the tissue TACs, ROIs were drawn on the image in Figure 2 and on the anterior, lateral, inferior and septal segments of the myocardium on the image in Figure 3. These five ROIs were copied onto measured image sequences (Figures 1a and 1b) and on sequences of blood pool and tissue to allow comparison and to show spillover effect. Figures 4 to 6 compare the input curve and the anterior and septal segments obtained from the raw reconstructed images and from the FADS structures components. For tissue TACs, the fit to the data obtained from FADS is also displayed.

The difference between the curves obtained from the original image series and those obtained from the FADS results can be explained by the spillover. Indeed, spillover should be at least partially compensated for using FADS, since in FADS, the total number of counts detected in a pixel can be distributed between several compartments. On the other hand, when deriving TACs from the original image series, one implicitely assumes that all pixels belonging to a specific ROI belong to a single compartment, and that in each pixel of the ROI, all signal is explained by a single compartment.

Regarding the input curve, it can be seen that the peak remains nearly unchanged (Figure 4b) but that the amplitude of the input curve obtained from FADS gets lower than that of the curve obtained from the original sequence as time increases (Figure 4a). This suggests that at later time, the blood pool ROI used in the analysis gets contaminated by counts coming from the tissue compartment. For the anterior and septal segments (Figures 5 and 6), the most affected regions of the curves are in the first frames which correspond to the higher uptake in the blood pool. The component extracted with FADS shows a significant spillover correction especially for the septal segment.

Table I reports the relative difference of total counts between raw image estimates and FADS for the input curve, the anterior and the septal segments calculated as 100 x (total of uncorrected – total FADS) / total of uncorrected, in the eight rats. These results suggest that spillover affects more the septal region than the anterior region in the myocardial tissue, and that the input fonction is also significantly affected by spillover. They also show that the two reconstruction methods yield different results, suggesting that the spillover issue depends on the algorithm used for reconstructing the images.

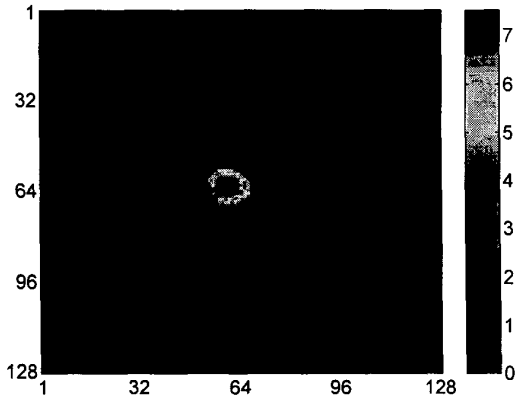

Figure 1a: Last frame image reconstructed with ML.

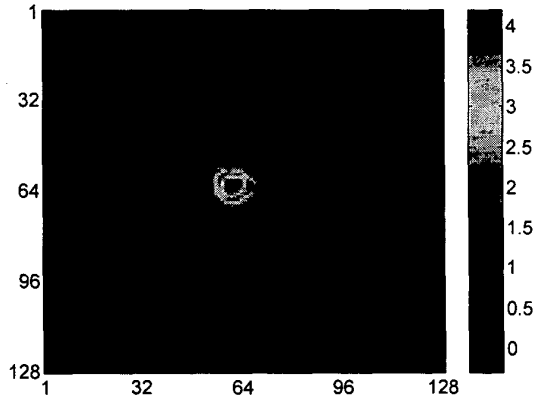

Figure 1b: Last frame image reconstructed with FBP.

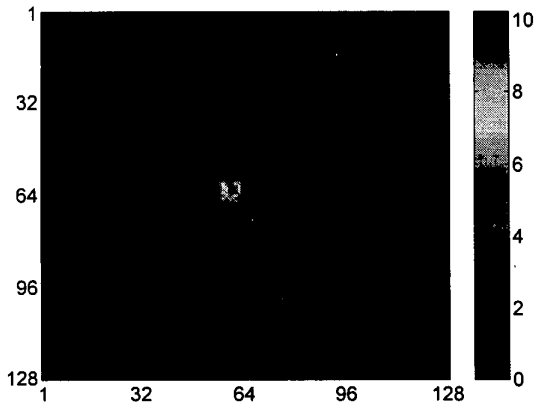

Figure 2: Image of blood pool component extracted from images reconstructed with ML.

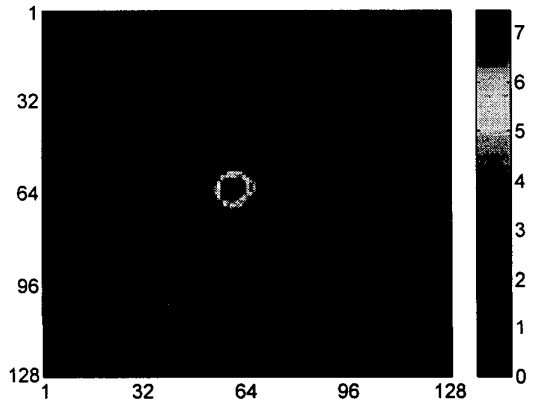

Figure 3: Image of myocardium tissue component extracted from images reconstructed with ML.

Such dependence could be caused by differences in spatial resolution depending on the reconstruction algorithm, and also by differences in noise propagation.

Since no external blood samples were available to estimate regional myocardial metabolic rates for glucose (rMMRGlc), no absolute values can be given in the present work. However, the relative difference between non-corrected input curve for spill-over and that obtained with FADS (Table 1) is expected to be observed (inversely) in rMMRGlc values obtained with these two input curves, since rMMRGlc and the integral of the input curve are inversely proportional.

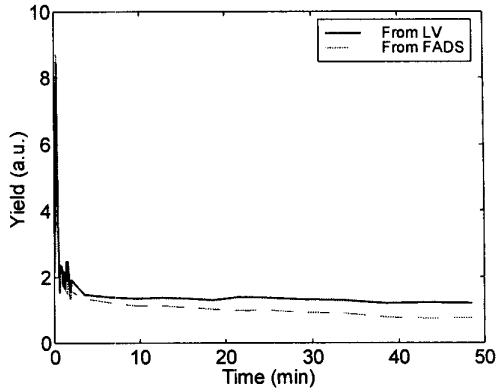

Figure 4a: Input curves obtained from ROIs defined on the LV cavity in measured images (Figure 1) and in blood pool images (Figure 2). The two curves coincide for earlier frames while the curve obtained with FADS is less contaminated by spill-over from the tissue for later frames.

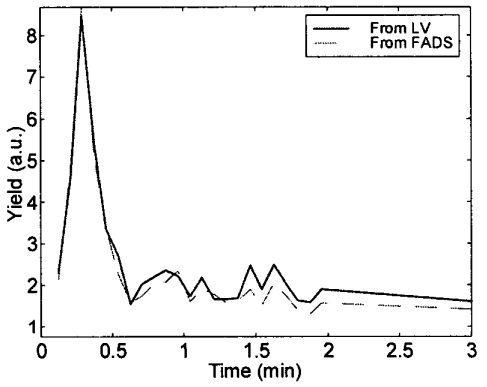

Figure 4b: Same as Figure 4a showing a close-up of the peak.

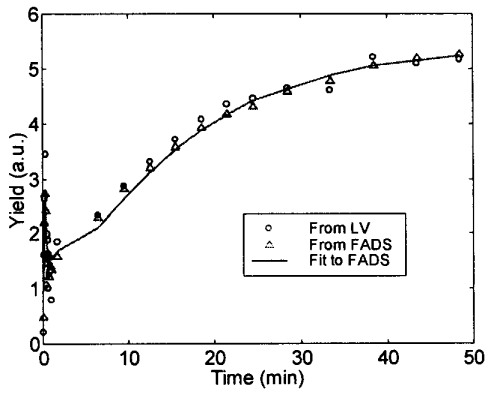

Figure 5: Anterior segment obtained from ROIs defined in measured images (Figure 1) and in tissue images (Figure 3). The spill-over from the blood pool affects tissue TAC at earlier frames only.

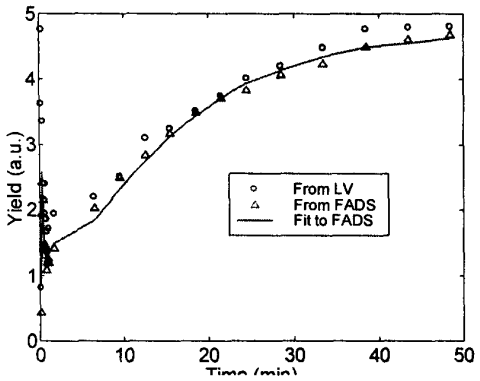

Figure 6: Septal segment obtained from ROIs defined in measured images (Figure 1) and in tissue images (Figure 3). Due to its small thickness and its position between the two blood cavities, the septum shows a higher amount of spill-over for the first frames, in comparison to the anterior segment (Figure 5).

Table I- Relative difference in total counts (in %) in the indicated ROIs obtained from measured data and from FADS images in each of the eight rats.

	Blood pool		Anterior		Septum	
Rat #	FBP	ML	FBP	ML	FBP	ML
1	16	21	48	20	53	42
2	14	33	33	15	57	48
3	31	7	21	23	24	43
4	12	21	28	18	24	43
5	20	23	38	28	58	48
6	38	13	18	21	25	46
7	17	13	35	23	51	52
8	25	10	14	3	24	19
Mean	22	18	29	19	39	43

IV. DISCUSSION

FADS technique was shown to be able to separate the blood pool from tissue in the left ventricle of rat hearts. The spill-over correction in both the input curve and tissue TACs allows to avoid external blood sampling and to simplify kinetic models when fitting tissue TAC. The spill-over correction in tissue can be observed in Figures 5 and 6, in the anterior and septal segments, respectively. The septum shows a higher amount of spill-over than the anterior segment, and after application of FADS, both these two segments show a peak of comparable intensity for the early frames. This peak represents the blood volume and is accounted for during the fitting procedure.

FADS is efficient in correcting for spill-over in a given structure, meanwhile statistical fluctuation in the pixel counts due to photon detection, image reconstruction techniques and cardiac movement may be accounted for as separate structures. Most kinetic models allow to fit for the residual spill-over not removed with FADS from tissue images. The feasibility of extracting the input curve from the left ventricle in human or in dogs using FADS has been demonstrated without adding specific constraints [6]. It has also been shown that FADS could properly estimate the input curve in small monkey using a single blood sample constraint [7]. Although the input functions estimated by FADS in our studies seem not to suffer from spillover as much as those obtained from raw images, the accuracy of these input functions still needs to be established by comparing FADS results with external input function measurements. The Sherbrooke small animal scanner allows generation of factor images without any constraint on the FADS algorithm, regardless of the image reconstruction method used.

V. CONCLUSIONS

The present study has demonstrated the feasibility of extracting blood input curve and myocardial tissue uptake from dynamic PET scans of rat heart using FADS. The proposed technique is being validated with quantitative PET scans, including external automatic blood sampling, for absolute determination of regional myocardial perfusion and glucose consumption using ammonia and FDG, the two most commonly used tracers in our center for cardiac rat studies.

VI. REFERENCES

[1] R. Lecomte et al., "Initial results from the Sherbrooke avalanche photodiode positron tomograph," IEEE Trans Nucl Sci, pp. 1952-1957, 1996.

[2] R. Di Paola et al., "Handling of dynamic sequences in nuclear medicine," IEEE Trans Nucl Sci, pp. 1310-1321,1982.

[3] M. Samal et al., "Enhancement of physiological factors in factor analysis of dynamic studies," Eur J Nucl Med, vol. 12, pp. 280-283, 1986.

[4] I. Buvat, "Correction de la diffusion en imagerie scintigraphique," Thesis, Université de Paris-Sud, Centre d'Orsay; 1992.

[5] V. Selivanov et al., "Detector response models for statistical iterative image reconstruction in high resolution PET", *1998 IEEE Nuclear Science Symposium & Medical Imaging Conference Record*, IEEE Catalog 98CH36255, vol. II, 1999, pp. 1377-1381.

[6] H. Wu et al., "Factor analysis for extraction of blood time-activity curves in dynamic FDG-PET studies," J Nucl Med, vol. 36, pp. 1714-1722, 1995.

[7] H. Wu et al., "Derivation of input function from FDG-PET studies in small hearts," J Nucl Med, vol. 37, pp. 1717-1722, 1996.